European Journal of Geography

The publication of the European Journal of Geography (EJG) is based on the European Association of Geographers' goal to make European Geography a worldwide reference and standard. Thus, the scope of the EJG is to publish original and innovative papers that will substantially improve, in a theoretical, conceptual, or empirical way the quality of research, learning, teaching, and applying geography, as well as in promoting the significance of geography as a discipline. Submissions are encouraged to have a European dimension. The European Journal of Geography is a peer-reviewed open access journal and is published quarterly.

Received: 23/09/2025
Revised: 20/12/2025
Revised: 12/02/2026
Accepted: 15/02/2026
Published: 21/02/2026

Editor:
Dr. Alexandros Bartzokas-Tsiompras

Research Article

Cluster Analysis of Neighborhood-Level Earthquake Risk Profiles in Istanbul: A Data-Driven Approach to a Magnitude 7.5 Mw Scenario

Rıdvan Avcı [1] **& Filiz Ersöz** [2]✉

[1] Department of Software Engineering, Ostim Technical University, Ankara, Türkiye
[2] Department of Management Information Systems, Ostim Technical University, Ankara, Türkiye

✉ Correspondence: filiz.ersoz@ostimteknik.edu.tr

Abstract: Urban seismic risk assessments in Istanbul have predominantly focused on district level loss estimates, even though mitigation and emergency response decisions are implemented at much finer administrative units. This study develops a neighborhood-based classification of earthquake risk for all 959 neighborhoods under a deterministic Mw 7.5 scenario. The analysis relies on the official Istanbul Earthquake Loss Estimation Update dataset prepared by Istanbul Metropolitan Municipality in cooperation with the Kandilli Observatory. Eight scenario-based outcome indicators, including four structural damage and four human impact variables, are first transformed using Yeo-Johnson and Min-Max scaling and then reduced through Principal Component Analysis, which explains 96.3 percent of the total variance in two components. Within this reduced space, K-Means, K-Medoids, Gaussian Mixture Models, Spectral Clustering, and HDBSCAN are systematically compared. Model selection is guided by internal validation criteria, the Gap Statistic, and bootstrap stability analysis. Based on this combined assessment, K-Medoids with k equal to 2 emerges as the most parsimonious and stable clustering solution. The resulting High Impact and Low Impact profiles show statistically significant differences across all indicators and remain highly consistent across 300 bootstrap resamples, with a mean Adjusted Rand Index of 0.976. The identified medoid neighborhoods provide concrete reference cases for targeted planning interventions. Spatially, higher impact areas are concentrated along the Marmara coastal corridor and older urban cores, whereas lower impact neighborhoods are more common in northern districts. By converting detailed scenario outputs into stable neighborhood level risk categories, the study provides a structured basis for prioritizing mitigation investments, preparedness actions, and emergency response planning at the local scale.

Keywords: Earthquake risk; Scenario-based loss estimation; Unsupervised learning; K-Medoids; Principal Component Analysis; Bootstrap ARI; Istanbul; Neighborhood-level

Highlights:

- Classified 959 Istanbul neighborhoods into data driven risk profiles under a Mw 7.5 scenario
- Compared five clustering algorithms and identified K-Medoids (k = 2) as the most consistent solution
- Demonstrated high cluster stability with a mean Adjusted Rand Index of 0.976
- Identified real medoid neighborhoods as actionable reference cases for planning

DOI: 10.48088/ejg.r.avc.17.1.017.034
ISSN: 1792-1341
E-ISSN: 2410-7433

1. Introduction

1.1. Background and motivation

Earthquakes rank among the most destructive natural hazards worldwide. When they affect large metropolitan regions, they can result in substantial loss of life, extensive physical damage, and prolonged socioeconomic disruption. With a population exceeding 16 million and a central role in Türkiye's economy, Istanbul is one of the most exposed cities in the Euro-Mediterranean region. Due to its proximity to the western termination of the North Anatolian Fault, the city faces a substantial probability of experiencing a major earthquake exceeding Mw 7.0 within the foreseeable future. Scenario studies suggest that, in the absence of effective risk mitigation measures, both expected annual losses and potential fatalities in Istanbul could increase considerably, highlighting the need for more evidence based and spatially refined risk reduction strategies.

In a megacity of this scale and complexity, earthquake risk is not spatially uniform. It arises from the combined effects of seismic hazard, exposure of population and assets, structural vulnerability of the building stock, and socioeconomic susceptibility. Local site conditions, building age and construction quality, population density, land use patterns, and accessibility may vary significantly not only across districts but even between adjacent neighborhoods. As a result, the internal geography of seismic risk in Istanbul is highly heterogeneous at the neighborhood scale.

This heterogeneity creates a practical challenge for planners and decision makers. While hazard and loss models often produce detailed technical outputs, policy implementation typically requires clear and interpretable categories that can be directly translated into priority lists, retrofitting programs, and emergency response strategies. This raises a practical question: how can detailed scenario-based loss estimates be synthesized, without losing essential information, into a limited number of robust neighborhood level risk profiles?

1.2. Istanbul loss-estimation studies and data-driven approaches

Seismic risk assessment in Istanbul has a well-established history. Early landmark studies by Erdik et al. (2003) and Ansal et al. (2009) integrated ground motion models, building inventories, and vulnerability functions to develop comprehensive damage and loss scenarios for the metropolitan area, producing deterministic and probabilistic loss estimates at regional and district scales. These efforts provided critical insights into potential damage distributions and substantially shaped risk awareness and policy discourse in Türkiye. At the district scale, Ersoz and Bayrak (2023) applied the Fine Kinney method to classify Istanbul's 39 districts using hazard proximity and building age proxies. While this approach provided a deterministic risk ranking framework, it did not incorporate official scenario-based loss outputs or formally evaluate the statistical robustness of the resulting classifications.

The present study advances beyond district level proxy-based scoring by synthesizing official neighborhood level scenario outputs and validating the clustering structure through multi criteria model selection and bootstrap stability assessment. However, early loss estimation studies were generally conducted at coarse spatial scales, such as districts or aggregated geographic cell clusters, and focused primarily on scenario specific loss figures rather than delivering data driven neighborhood typologies or risk profiles. While subsequent work improved hazard modeling for the Marmara Region (e.g., Kalkan et al., 2009) and advanced urban loss estimation tools such as ELER (Erdik et al., 2010), the primary outputs largely remained expected damage and fatality maps rather than stable neighborhood level classes designed for operational prioritization.

In parallel, the international literature has increasingly adopted machine learning and clustering techniques to uncover latent structure in multidimensional risk indicators, as illustrated by post Wenchuan resilience assessments in China (Li et al., 2016), the identification of seismic hot spots in Palu, Indonesia (Jena et al., 2020), and the delineation of seismic hazard zones in Mexico City (Olivares-Palomares et al., 2025). In the Istanbul context, data driven neighborhood scale studies on social vulnerability and resilience have also begun to emerge (Ghaffarian et al., 2025; Kalaycıoğlu et al., 2023).

Despite these advances, three core gaps remain salient for Istanbul:

- Scale and resolution: Many studies continue to rely on district level aggregates, which can mask substantial within district spatial heterogeneity and limit the usability of results for neighborhood level interventions.

https://doi.org/10.48088/ejg.r.avc.17.1.017.034

- Methodological rigor: Clustering analyses are often implemented with a single algorithm and a fixed number of clusters, without systematic comparison of alternative models or quantitative assessment of cluster stability.
- Operational interpretability: The linkage between statistical clusters and operational constructs, such as prioritized neighborhoods for retrofitting programs or the pre-positioning of emergency response resources, is not always articulated in a clear and actionable manner.

Existing studies on Istanbul have not yet systematically synthesized official scenario-based loss outputs into neighborhood scale risk groupings that are both evaluated for internal quality and tested for robustness against sampling variability. Rather than operating at a coarser scale, the present study deliberately shifts the analytical focus to the neighborhood level, where emergency response and mitigation decisions are implemented in practice.

1.3. Objectives and contributions

Building on an up to date, citywide dataset produced by Istanbul Metropolitan Municipality and the Kandilli Observatory for a deterministic Mw 7.5 nighttime earthquake scenario, this study addresses the limitations outlined above. By adopting the neighborhood as the unit of analysis, it aims to derive risk profiles that are both statistically robust and operationally interpretable.

The study makes four principal contributions.

1. Neighborhood scale classification based on current scenario data. Official loss estimation outputs are employed for all 959 neighborhoods of Istanbul under the Mw 7.5 scenario, capturing both structural damage and human impacts. While earlier studies such as Erdik et al. (2003) and Ansal et al. (2009) provided district-level loss estimates, the present analysis explicitly focuses on the neighborhood as the primary decision scale.
2. Robust multi criteria model selection. An integrated preprocessing pipeline combined with Principal Component Analysis is followed by a systematic comparison of five clustering algorithms: K-Means, K-Medoids, Gaussian Mixture Models, Spectral Clustering, and HDBSCAN. The number of clusters is determined through a combined evidence framework that synthesizes internal validation indices together with the Gap Statistic.
3. Formal stability assessment of risk profiles. Cluster stability is evaluated through bootstrap resampling with 300 iterations and analysis of the Adjusted Rand Index. This procedure extends prior studies that report a single clustering solution without examining robustness to sampling variability or sensitivity to initialization.
4. Medoid based prototypes for planning applications. By employing K-Medoids, the analysis identifies actual neighborhoods as representative prototypes for each risk profile. This facilitates the translation of statistical groupings into concrete reference areas for retrofitting prioritization and emergency planning.

Overall, the study complements physically based loss assessment efforts such as Erdik et al. (2003) and Ansal et al. (2009) by leveraging the most recent official scenario data to produce a rigorously validated and data driven classification tailored to neighborhood scale risk management in Istanbul.

2. Study Area

2.1. Geographic and urban context

Located in northwestern Türkiye, Istanbul extends across both sides of the Bosporus Strait, connecting Europe and Asia. The city is bordered by the Black Sea to the north and the Sea of Marmara to the south. Administratively, Istanbul is divided into 39 districts and 959 neighborhoods, which represent the smallest operational units for several municipal services and emergency management functions. The overall boundaries of the study area, together with the fault geometry of the deterministic Mw 7.5 scenario adopted in the Istanbul Province Possible Earthquake Loss Estimates Update Project, are presented in Figure 1. The project was initiated in 2019, and its outputs were disseminated between 2019 and 2023.

The city exhibits pronounced contrasts in its urban structure and socioeconomic conditions. Districts along the Sea of Marmara coastline are characterized by dense residential and mixed-use areas, where a substantial proportion of the building stock predates 2000. In contrast, northern districts are dominated by more recent developments, extensive forested zones, and critical lifelines such as water reservoirs and energy transmission corridors. Because risk distributions may vary significantly even within district boundaries, this internal heterogeneity makes neighborhood scale analysis particularly important.

https://doi.org/10.48088/ejg.r.avc.17.1.017.034

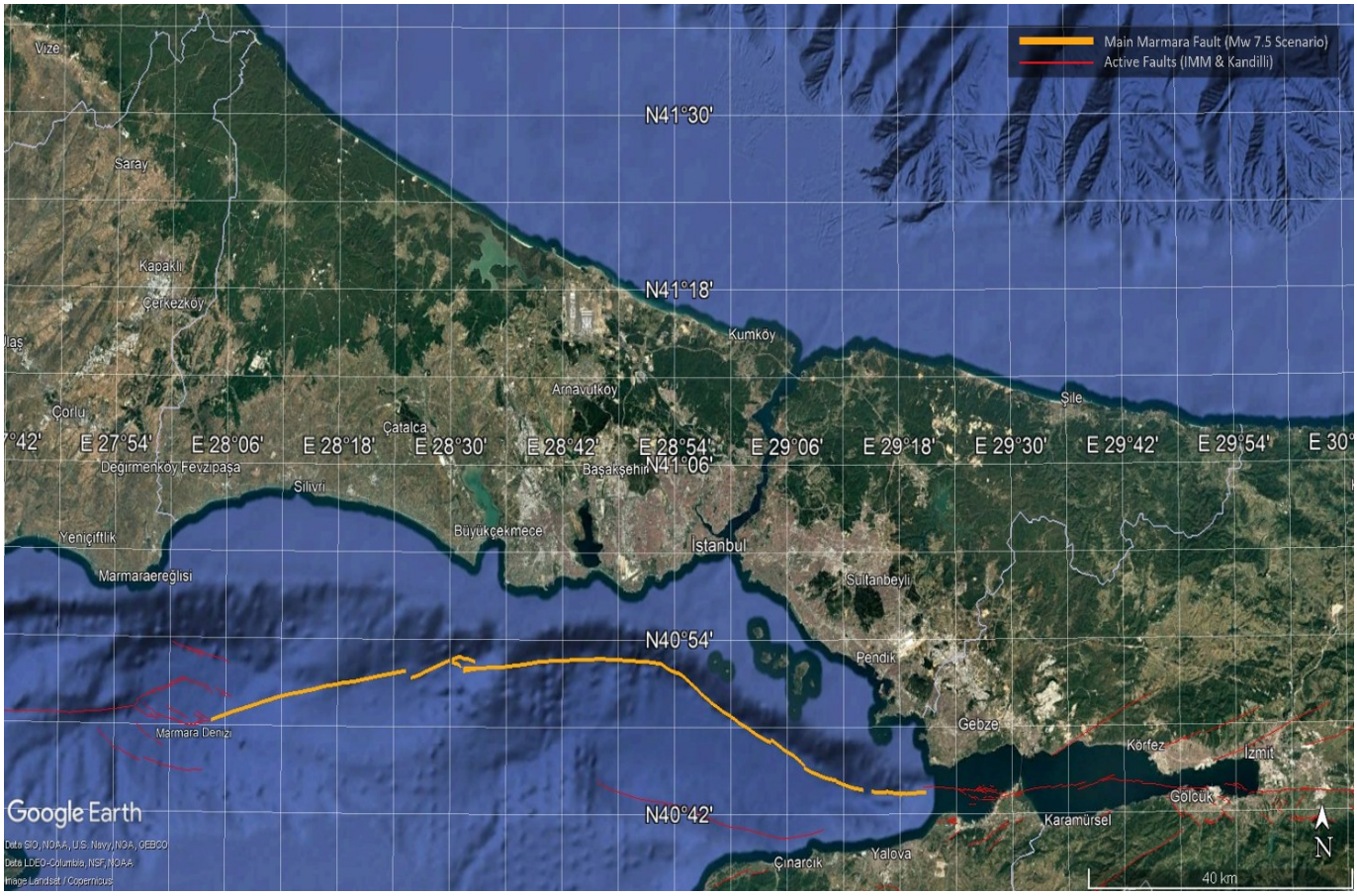

Figure 1. Tectonic setting of the Sea of Marmara showing the active fault system (thin red lines) and the assumed rupture trace for the deterministic Mw 7.5 earthquake scenario (thick orange line) based on the IMM and Kandilli dataset (Map base: Google Earth Pro).

2.2. Geological setting and seismic history

Istanbul's seismic risk is primarily governed by the North Anatolian Fault system, particularly the offshore Marmara segments located to the south of the city. Geophysical and seismological research indicates a substantial probability that one or more of these segments may rupture in a major event with a moment magnitude in the range of 7.2 to 7.5. Local site conditions display marked spatial variability, ranging from soft alluvial deposits and artificial fill along the Sea of Marmara coastal corridor, including Avcılar, Zeytinburnu, and parts of Fatih and Bakırköy, to more competent rock formations that characterize much of the northern districts.

Historical earthquakes—most notably the 1999 Kocaeli and Düzce events—have demonstrated that basin effects, site amplification, and nonlinear soil response can strongly influence damage patterns in Istanbul, even at considerable distances from the epicenter. These geological and historical characteristics provide the physical framework within which the Mw 7.5 IMM scenario adopted in this study, as well as the ensuing clustering analysis, should be interpreted.

3. Materials and Methods

The methodological framework follows a structured analytical pipeline consisting of four main stages: (i) compilation and summarization of scenario-based loss estimates at the neighborhood-level, (ii) statistical preprocessing and dimensionality reduction, (iii) comparative clustering analysis, and (iv) multi stage robustness assessment.

The logical structure of the research design and the sequential implementation of each analytical component are summarized in Figure 2.

https://doi.org/10.48088/ejg.r.avc.17.1.017.034

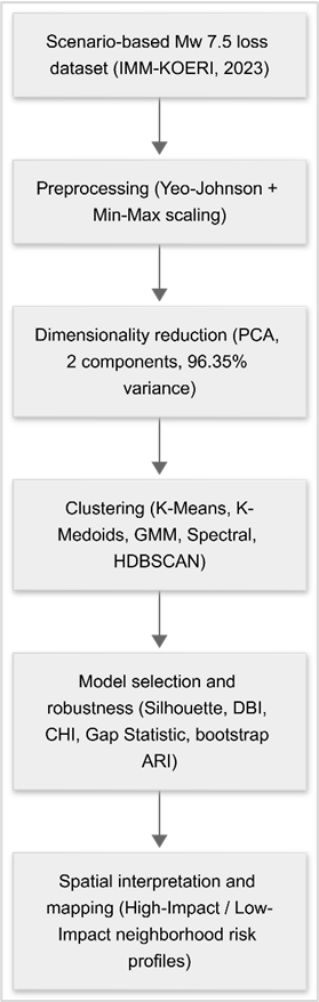

Figure 2. Methodological workflow from the Mw 7.5 scenario-based loss dataset to neighborhood-level clustering, robustness assessment, and spatial interpretation of High-Impact and Low-Impact risk profiles.

3.1. Scenario-based loss dataset

3.1.1. Earthquake scenario and loss-estimation framework

The primary data source for this study consists of the neighborhood level outputs of the Istanbul Province Possible Earthquake Loss Estimates Update Project, initiated in 2019 and disseminated between 2019 and 2023. The project was conducted by Istanbul Metropolitan Municipality in collaboration with the Boğaziçi University Kandilli Observatory and Earthquake Research Institute. It evaluates a deterministic Mw 7.5 nighttime scenario representing a major rupture on the Marmara segment of the North Anatolian Fault. Public technical documentation describing the scenario definition, modeling workflow, and reporting structure is available through the official Deprem Zemin project pages and the accompanying district loss estimate booklets.

According to the Deprem Zemin documentation, loss estimation is generated through an integrated sequence of hazard modeling, exposure compilation, vulnerability characterization, and loss calculation. In the hazard module, scenario specific ground motion fields are produced and adjusted for local site conditions. The exposure stage classifies the building stock by typology, height, and construction period. Vulnerability relationships link spectral demand to discrete damage state probabilities, which are subsequently combined with nighttime occupancy assumptions to estimate human impacts at fine spatial resolution. This modular structure aligns with established Istanbul loss estimation implementations while reflecting updated inventories and reporting standards in the 2019 to 2023 project.

https://doi.org/10.48088/ejg.r.avc.17.1.017.034

In the present study, these official outputs are treated as exogenous scenario-based impact indicators rather than as a model to be re-estimated. We therefore do not rerun the underlying hazard, exposure, vulnerability, or loss modules. Instead, the reported neighborhood level outcomes are statistically synthesized to derive a stable and operationally interpretable typology. The dataset provides expected counts for eight outcome variables, comprising four building damage state indicators and four injury and fatality indicators for all 959 neighborhoods. This enables a citywide and internally consistent comparison at the finest administrative level routinely used in municipal and emergency management operations. The indicators are documented in a standardized reporting format across districts and neighborhoods, ensuring transparent traceability from the scenario definition to the officially reported loss outputs.

Accordingly, uncertainties associated with the physical modeling stages are inherited from the official scenario framework. The focus of the present analysis is therefore on the statistical synthesis and interpretation of the reported loss indicators rather than on re estimating the underlying physical processes.

3.1.2. Neighborhood-level indicators

For each of Istanbul's 959 neighborhoods, the IMM scenario reports expected counts for four building damage states and four injury and fatality categories under the Mw 7.5 nighttime scenario. These eight variables serve as clustering inputs and are grouped into two conceptual dimensions (see Table 1).

Structural damage indicators

- Bina_1: Slightly damaged buildings
- Bina_2: Moderately damaged buildings
- Bina_3: Severely damaged buildings
- Bina_4: Collapsed buildings

Human-impact indicators

- HumanImpact_1: Slightly injured individuals
- HumanImpact_2: Hospitalized individuals
- HumanImpact_3: Severely injured individuals
- HumanImpact_4: Fatalities

Neighborhoods without reported values in a given category are treated as having zero expected impact for that category, consistent with the reporting structure of the official scenario dataset.

Table 1. Eight neighborhood-level indicators derived from the Mw 7.5 scenario and their brief descriptions.

Indicator group	**Code**	**Description (neighborhood-level under Mw 7.5 nighttime scenario)**	**Unit**
Structural-damage indicators	Bina_1	Expected number of slightly damaged buildings in the neighborhood	Count of buildings
Structural-damage indicators	Bina_2	Expected number of moderately damaged buildings in the neighborhood	Count of buildings
Structural-damage indicators	Bina_3	Expected number of severely damaged buildings in the neighborhood	Count of buildings
Structural-damage indicators	Bina_4	Expected number of collapsed buildings in the neighborhood	Count of buildings
Human-impact indicators	HumanImpact_1	Expected number of slightly injured residents in the neighborhood	Count of people
Human-impact indicators	HumanImpact_2	Expected number of hospitalized (non-critical) injured residents in the neighborhood	Count of people
Human-impact indicators	HumanImpact_3	Expected number of severely injured residents in the neighborhood	Count of people
Human-impact indicators	HumanImpact_4	Expected number of fatalities in the neighborhood	Count of people

https://doi.org/10.48088/ejg.r.avc.17.1.017.034

The neighborhood is adopted as the unit of analysis, reflecting both the spatial resolution of the loss estimates and the operational scale of many municipal and emergency-management decisions.

3.2. Preprocessing and dimensionality reduction

The eight outcome variables exhibit substantial positive skewness and strong intercorrelations. For example, neighborhoods with high expected fatalities typically also report high counts of extensively damaged buildings. Applying distance based clustering algorithms directly to such data may lead to solutions dominated by high magnitude variables and influenced by multicollinearity among indicators.

To address these issues, a two-step transformation procedure was implemented:

- **Yeo–Johnson transformation**: A univariate Yeo–Johnson power transformation was applied to each variable to reduce right skewness and stabilize variance while accommodating zero valued observations (Yeo & Johnson, 2000).
- **Min–Max scaling**: The transformed variables were subsequently rescaled to the interval between 0 and 1 to ensure that each indicator contributes comparably to Euclidean distance calculations in the clustering stage.

Following preprocessing, Principal Component Analysis (PCA) was applied to mitigate multicollinearity and project the dominant variation into a lower dimensional space (Jolliffe, 2002). For clustering, the first two principal components were retained. Together, they explain 96.3 percent of the total variance (PC1: 89.7 percent; PC2: 6.6 percent; see Table 2). All eight indicators load positively and strongly on the first component, indicating that it represents an overall impact dimension combining structural damage and human losses. The second component captures secondary contrasts between structural damage and human impact variables. Because PCA is employed primarily as a dimensionality reduction step prior to clustering, detailed interpretation of individual loadings is not emphasized here.

Table 2. Summary of the first two principal components used for clustering (explained variance and qualitative interpretation)

Component	Explained variance (%)	Cumulative variance (%)	Interpretation
PC1	89.7	89.7	Overall impact (building damage + casualties)
PC2	6.6	96.3	Damage vs. human-impact contrast

3.3. Clustering algorithms and model selection

Clustering analysis was carried out in the two-dimensional space defined by the first two principal components to examine the dominant structure of the data under reduced dimensionality. To mitigate algorithm specific bias and to evaluate the robustness of the inferred grouping, five clustering methods representing complementary paradigms, namely prototype based, probabilistic, graph based, and density-based approaches, were applied (Jain, 2010; Xu & Wunsch, 2005).

The set of algorithms included K-Means as a classical centroid based partitioning approach (MacQueen, 1967) and K-Medoids, also known as Partitioning Around Medoids, as a medoid based alternative that is less sensitive to extreme observations (Kaufman & Rousseeuw, 1990). Gaussian Mixture Models were employed to represent a model-based perspective in which clusters are assumed to arise from a mixture of underlying probability distributions (Fraley & Raftery, 2002). In addition, Spectral Clustering was used to identify potential nonlinear or non-convex structures through a graph-based representation of similarity (Ng et al., 2002), while HDBSCAN was applied as a density-based method capable of detecting clusters with heterogeneous densities and explicitly identifying noise points (Campello et al., 2015).

For clustering algorithms requiring the number of clusters to be specified a priori, candidate solutions were generated for values of k ranging from 2 to 6. The quality of these solutions was assessed using multiple internal validation criteria capturing complementary aspects of clustering performance. Specifically, the Silhouette coefficient was used to evaluate the balance between within cluster cohesion and between cluster separation (Rousseeuw, 1987). The Davies Bouldin Index was employed as a measure of average cluster similarity, with lower values indicating more distinct and compact clusters (Davies & Bouldin, 1979). In addition, the Calinski Harabasz Index was used to quantify the ratio of

between cluster dispersion to within cluster dispersion, where higher values suggest stronger separation between clusters (Calinski & Harabasz, 1974).

To further support the determination of an appropriate number of clusters, the Gap Statistic was applied to compare the observed clustering solutions with those obtained from a null reference distribution lacking inherent cluster structure (Tibshirani et al., 2001). The one standard error rule was adopted to favor more parsimonious solutions when multiple values of k exhibited comparable performance, thereby reducing the risk of over partitioning.

Although five clustering algorithms were initially examined, only the partition-based approaches (K-Means and K-Medoids) generated solutions that were both statistically competitive and operationally consistent with the study objective. Gaussian Mixture Models and Spectral Clustering exhibited comparatively lower Silhouette values and higher Davies–Bouldin indices across candidate solutions. In addition, HDBSCAN assigns low-density observations to a noise category (cluster −1), thereby producing non-exhaustive partitions. Because the analytical framework requires the allocation of every administrative neighborhood to a clearly defined risk group, this characteristic limited its practical suitability. Accordingly, detailed validation metrics for these alternative methods are not reported, in order to preserve analytical focus and interpretability.

Internal validation results for the K-Means and K-Medoids algorithms across values of k equal to 2 through 6 are summarized in Table 3. For both algorithms, the two cluster solutions achieved the highest Silhouette values and the lowest Davies Bouldin scores, indicating strong within cluster cohesion and clear separation between clusters. As the number of clusters increased, Silhouette coefficients declined steadily while Davies Bouldin values increased, suggesting a gradual deterioration in clustering quality for more complex solutions. Although Calinski Harabasz values increased markedly for the six cluster solutions, this increase was not accompanied by corresponding improvements in Silhouette or Davies Bouldin values.

This pattern is consistent with the known tendency of the Calinski Harabasz Index to favor larger numbers of clusters and therefore does not necessarily reflect a substantively superior clustering structure. Across nearly all values of k, K-Medoids produced slightly higher Silhouette scores and lower Davies Bouldin values than K-Means, suggesting greater robustness to potential outliers in the PCA space. Taken together, the convergence of evidence from multiple internal validation metrics and the Gap Statistic supports the selection of a two-cluster solution as the most stable, parsimonious, and interpretable representation of the underlying data structure.

Table 3. Internal validation metrics for K-Means and K-Medoids solutions with k equal to 2 through 6 in PCA space

k	Algorithm	Silhouette	DBI	CHI
2	K-Medoids	0.5928	0.5518	1370.8611
2	K-Means	0.5925	0.5564	1399.9934
3	K-Medoids	0.5612	0.5948	1038.2280
3	K-Means	0.5576	0.6039	1014.6880
4	K-Medoids	0.5293	0.6427	859.5427
4	K-Means	0.5203	0.6533	835.9061
5	K-Medoids	0.5034	0.6886	768.3052
5	K-Means	0.4919	0.7044	750.3005
6	K-Medoids	0.4430	0.7592	2421.2203
6	K-Means	0.4270	0.7764	2466.2780

3.4. Robustness and stability assessment

The analysis extends beyond internal validity metrics by evaluating the stability of candidate clustering solutions through bootstrap resampling and consensus analysis.

Bootstrap ARI: For each algorithm and each value of k, B equal to 300 bootstrap samples were generated by resampling neighborhoods with replacement. The clustering algorithm was re-estimated for every bootstrap sample,

and the resulting partitions were compared with the baseline solution using the Adjusted Rand Index, ARI (Hubert & Arabie, 1985). Higher mean ARI values indicate stronger agreement with the original partition and therefore greater structural robustness under sampling variability.

Seed sensitivity: For algorithms that depend on random initialization, such as K-Means and K-Medoids, repeated runs were conducted using different random seeds. The variability of internal validation metrics across these runs was examined to assess the extent to which results were influenced by initial conditions.

Consensus matrix: To detect stable grouping patterns and identify borderline assignments, a consensus matrix was constructed and visualized. This matrix summarizes the proportion of bootstrap iterations in which pairs of neighborhoods were assigned to the same cluster (Monti et al., 2003; Von Luxburg, 2010). High consensus values indicate consistently co-clustered observations, whereas lower values suggest instability or ambiguous membership.

Together, these complementary procedures ensure that the selected clustering solution is not only well separated according to internal evaluation criteria but also reproducible under sampling variation and resilient to algorithmic randomness.

4. Results

4.1. Structure of the PCA space

Principal Component Analysis was performed on the eight preprocessed outcome indicators to identify the dominant latent dimensions governing the data structure. The first two principal components jointly account for 96.3 percent of the total variance, with PC1 explaining 89.7 percent and PC2 explaining 6.6 percent of the variance, as illustrated in Figure 3. This high cumulative proportion indicates that the multivariate configuration of the dataset can be adequately represented within a two dimensional space without substantial information loss.

The loading pattern of PC1 reveals consistently strong positive contributions from all indicators. This uniform directionality suggests that PC1 captures a general severity dimension and can therefore be interpreted as a global impact axis summarizing the overall magnitude of expected structural damage and human losses at the neighborhood level. Neighborhoods positioned at the upper end of this axis correspond to areas with elevated expected counts of damaged buildings and fatalities under the Mw 7.5 scenario, whereas those located at the lower end represent comparatively lower impact profiles.

In contrast, PC2 explains a smaller but still meaningful portion of total variance and reflects variation in the relative composition of impacts rather than their absolute magnitude. Specifically, this component differentiates neighborhoods according to the balance between structural damage indicators and human loss indicators. As such, PC2 captures secondary structural contrasts that are not fully described by the dominant severity gradient represented by PC1.

Together, the configuration defined by PC1 and PC2 provides a parsimonious yet comprehensive representation of the impact landscape, forming an analytically appropriate input space for subsequent clustering procedures.

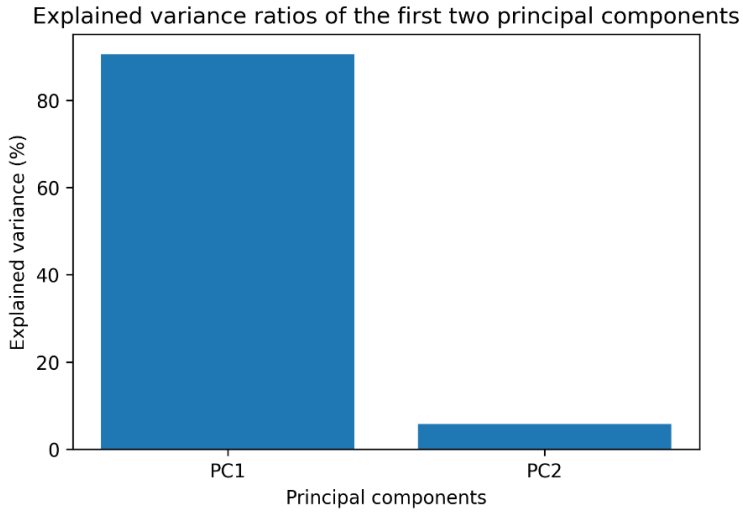

Figure 3. Explained variance ratios of the first two principal components used as input space for clustering.

https://doi.org/10.48088/ejg.r.avc.17.1.017.034

4.2. Algorithm comparison and choice of k

Across the evaluated methods, partition-based algorithms, namely K-Means and K-Medoids, achieved stronger internal validity than the spectral and density-based approaches for this dataset. This difference was consistently reflected in higher Silhouette values and lower Davies Bouldin values across the examined k range. Accordingly, the comparison of cluster solutions focuses on the two partition-based methods.

Between them, K-Medoids offers two practical advantages. First, its internal validation scores are comparable to, and in most cases slightly better than, those obtained with K-Means. Second, cluster centers are defined by actual neighborhoods rather than abstract centroids. This property enhances interpretability and facilitates direct inspection of representative profiles (Kaufman & Rousseeuw, 1990).

Evaluation of candidate solutions across k values equal to 2 through 6 indicates that clustering quality is highest at k equal to 2. The Silhouette coefficient reaches its maximum at this level and declines steadily as the number of clusters increases. The Davies Bouldin Index shows the same pattern, attaining its minimum at k equal to 2 and worsening for larger k values. Although the Calinski Harabasz Index increases at higher k levels, this rise is not accompanied by improvements in separation and compactness according to the other indices, and therefore does not provide sufficient support for adopting a more complex partition.

The Gap Statistic exhibits a local maximum around k = 4, indicating a potential secondary sub-structure in the data. However, when evaluated alongside the one-standard-error (1-SE) rule and bootstrap resampling, the k = 4 solution shows reduced assignment consistency, suggesting that the additional partitions are not reliably reproducible. In contrast, the parsimonious k = 2 configuration maintains a mean assignment stability exceeding 98%, demonstrating superior robustness to sampling variability. Therefore, to avoid unnecessary subdivision and to ensure distinct, operationally reproducible risk profiles, the statistically most stable two-cluster solution was selected as the final model.

On this basis, the selection of k equal to 2 reflects a convergence of internal validation evidence rather than an arbitrary choice. More detailed partitions introduce additional segmentation but do not yield substantively stronger or more interpretable group structures. From a planning perspective, the two-cluster solution also provides a clear and operationally meaningful distinction between higher impact and lower impact neighborhoods, whereas higher k solutions generate finer subdivisions without consistent empirical support.

4.3. Stability of the clustering solution

The robustness of the final K-Medoids solution with k equal to 2 was assessed using bootstrap resampling with B equal to 300 and consensus analysis. Across bootstrap samples, the Adjusted Rand Index values remain highly concentrated near 1, indicating strong agreement with the baseline partition. The mean ARI is 0.976 and the median is 0.980. The range between the 5th and 95th percentiles extends from 0.935 to 1.000, reflecting limited dispersion across resamples. The empirical distribution of these ARI values is presented in Figure 4.

Silhouette values computed under different random seeds exhibit negligible variation, suggesting that the two-cluster configuration is not sensitive to initialization conditions. This consistency indicates that the observed partition is not driven by algorithmic randomness.

Additional evidence is provided by the consensus matrix derived from the bootstrap replications. The matrix reveals a clear block structure, with co assignment frequencies exceeding 99 percent within both clusters. Neighborhood pairs that belong to the same cluster in the baseline solution remain grouped together in nearly all bootstrap iterations. The corresponding consensus matrix is shown in Figure 5.

Taken together, these findings indicate that the binary partition distinguishing High Impact and Low Impact neighborhoods represents a stable structural pattern in the scenario data. The solution remains reproducible under resampling and robust to initialization variability.

4.4. Cluster profiles and spatial patterns

With k equal to 2, the final K-Medoids solution partitions the 959 neighborhoods of Istanbul into two interpretable groups: a High Impact cluster with 503 neighborhoods and a Low Impact cluster with 456 neighborhoods. Cluster spe-

https://doi.org/10.48088/ejg.r.avc.17.1.017.034

cific mean values for the eight neighborhood level indicators, expressed in their original measurement units, are reported in Table 4. The reported means indicate consistent separation between the two profiles across both structural damage and human impact indicators.

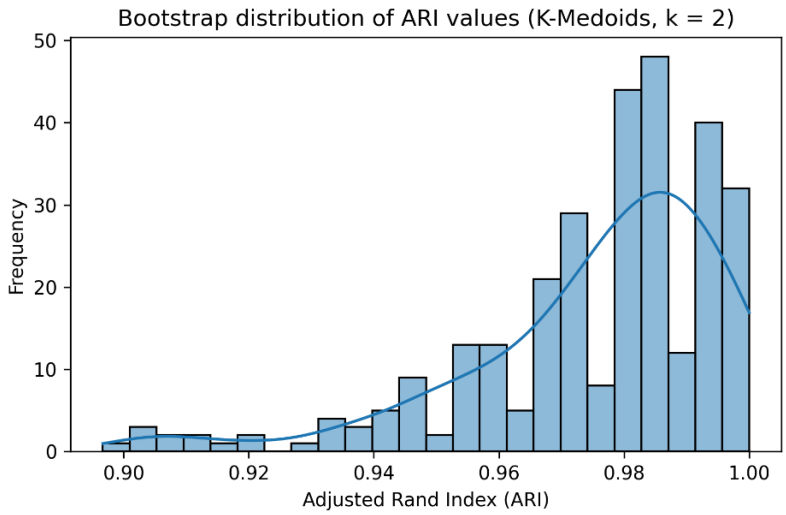

Figure 4. Bootstrap distribution of Adjusted Rand Index (ARI) values for the K-Medoids solution with k = 2 (B = 300 resamples).

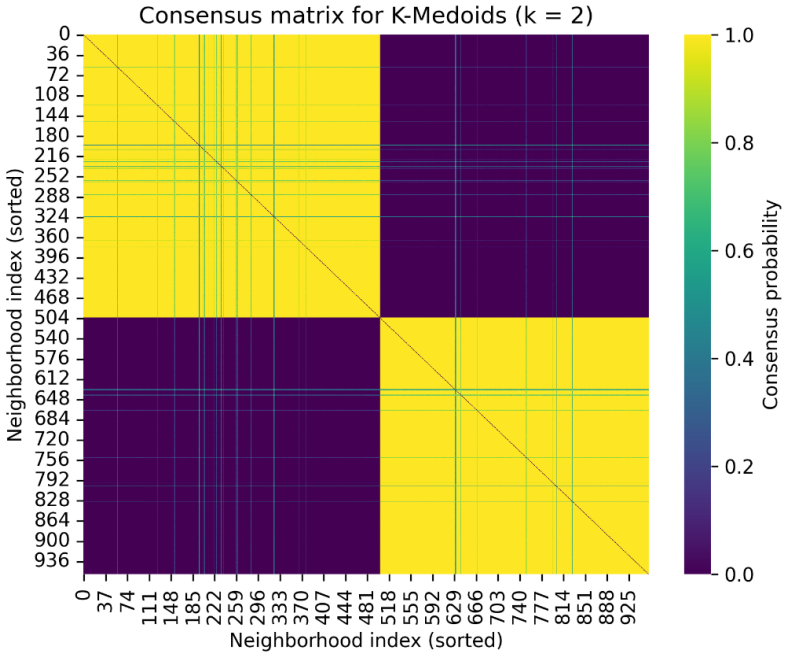

Figure 5. Consensus matrix for the K-Medoids solution with k = 2, showing the frequency with which pairs of neighborhoods are assigned to the same cluster across bootstrap resamples.

Across all eight outcomes, the High Impact cluster exhibits substantially larger than expected values. For structural damage variables, neighborhoods in Cluster 0 show markedly higher averages for moderate and heavy damage indicators as well as collapsed buildings compared with Cluster 1. A similar pattern is observed for all human impact measures, including expected fatalities and injury related outcomes. These differences indicate that, under the Mw 7.5 scenario, Cluster 0 represents neighborhoods exposed to systematically higher expected consequences, whereas Cluster 1 corresponds to comparatively lower impact areas.

https://doi.org/10.48088/ejg.r.avc.17.1.017.034

To formally assess the separation between clusters, nonparametric Mann-Whitney U tests were conducted for each indicator. All eight comparisons yielded $p < 10^{-6}$. Effect sizes computed using Cliff delta range approximately between 0.81 and 0.99, indicating strong separation in practical as well as statistical terms. Detailed test statistics are provided in the Appendix (Table A1).

Spatially, the two profiles exhibit a clear geographic structure. High Impact neighborhoods are concentrated along the Sea of Marmara coastal corridor and within older and denser urban zones. In contrast, Low Impact neighborhoods are more prevalent in northern districts characterized by relatively newer development and more favorable site conditions. The neighborhood level classification is visualized in Figure 6, where each point corresponds to a specific neighborhood. The map shows that High Impact areas form a contiguous belt along the Marmara coastline rather than appearing randomly scattered across the city.

This spatial configuration aligns with established geological patterns. Coastal areas are associated with alluvial deposits and artificial fill zones that amplify ground motion, whereas northern districts are more frequently located on stiffer soil or rock formations. The resulting north south gradient reflects the combined influence of building stock characteristics and local site conditions on expected impact levels.

Table 4. Cluster-wise mean values of the eight neighborhood-level indicators (raw units; see Table 1 for indicator definitions).

Indicator	High-Impact (Cluster 0) Mean	Low-Impact (Cluster 1) Mean
Bina_1	24.36	0.49
Bina_2	111.04	13.14
Bina_3	99.01	12.69
Bina_4	4.01	0.10
HumanImpact_1	27.68	3.18
HumanImpact_2	164.55	18.58
HumanImpact_3	34.41	4.72
HumanImpact_4	0.78	0.06

4.5. Medoid neighborhoods as prototypes

An advantage of the K-Medoids approach is that cluster centers correspond to actual observations rather than abstract centroids. In the final solution with k equal to 2, each profile is represented by a specific neighborhood selected as the medoid.

The medoid of the High Impact cluster is Fatih district, Nişanca neighborhood. Located within the Historic Peninsula, Nişanca is characterized by dense urban fabric, relatively older building stock, and high occupancy levels. These features align with the broader structural and human impact patterns observed in the High Impact cluster, making it a representative case of neighborhoods with elevated expected consequences.

The medoid of the Low Impact cluster is Çekmeköy district, Sultançiftliği neighborhood. This area reflects comparatively newer development patterns, lower building density, and more favorable site conditions. Its indicator profile closely matches the overall characteristics of the Low Impact cluster.

Identifying real neighborhoods as cluster representatives has practical implications. The medoids serve as concrete reference points for policy design and field level interventions. Detailed assessments, pilot retrofitting programs, and community-based planning initiatives can initially be implemented in these representative neighborhoods and subsequently extended to other members of the same cluster.

5. Discussion

5.1. Added value relative to prior Istanbul loss studies

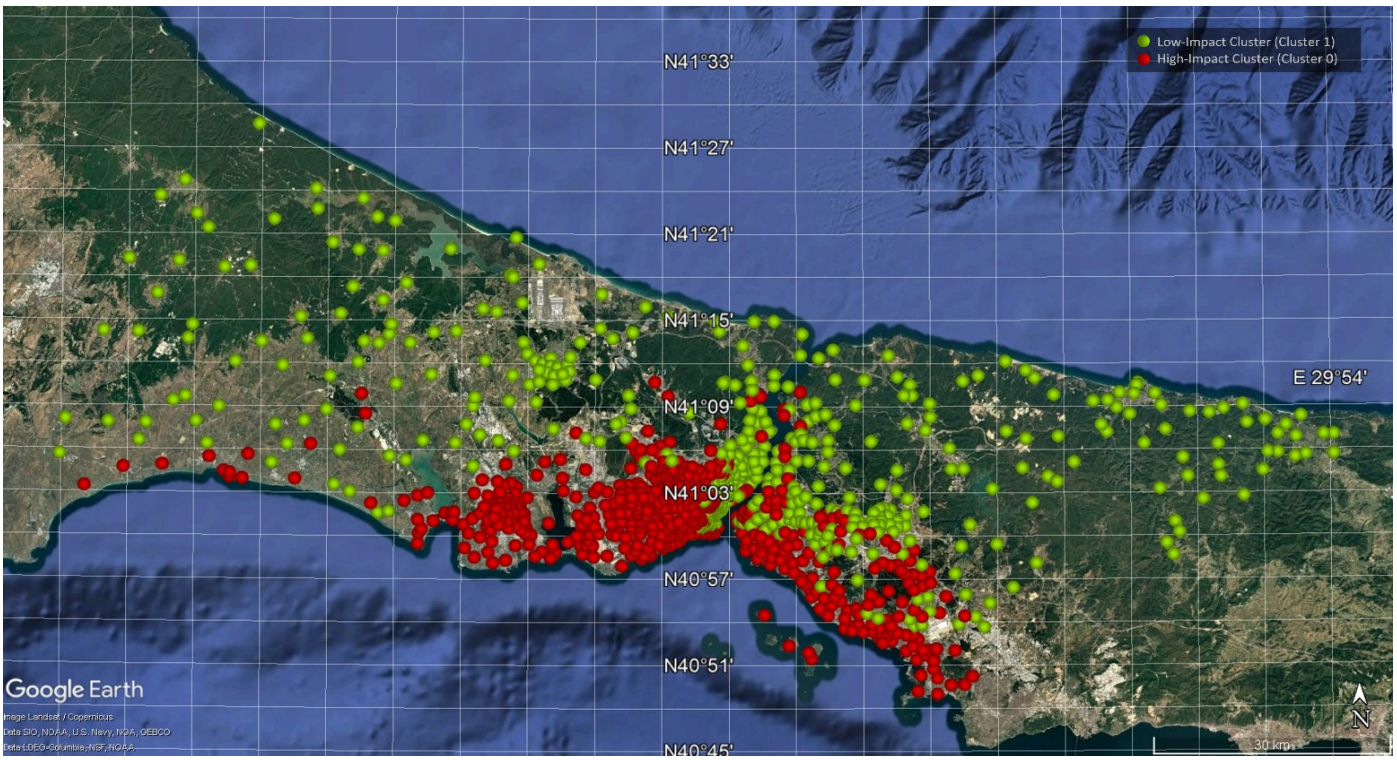

Figure 6. Neighborhood level spatial distribution of earthquake impact profiles. Red points represent High Impact neighborhoods and green points represent Low Impact neighborhoods. Each point corresponds to one of the 959 neighborhoods and the visualization does not aggregate results at the district scale. Base map: Google Earth Pro.

Early Istanbul focused earthquake loss studies, particularly those conducted by Erdik et al. (2003) and Ansal et al. (2009), provided comprehensive scenario-based damage and loss estimations and substantially shaped subsequent risk awareness and policy debates. Erdik et al. (2003) developed metropolitan scale scenarios grounded in intensity and spectral displacement frameworks. Ansal et al. (2009) extended this line of work through deterministic ground motion modeling and refined site response analyses for the Marmara Region.

The present study does not attempt to reproduce the physically detailed modeling structure of these earlier investigations. Instead, it builds upon their analytical foundation in two main respects. First, it utilizes a more recent and citywide loss dataset disseminated through the Deprem Zemin project and the associated district level reports published by the Istanbul Metropolitan Municipality. This dataset incorporates updated hazard representations, building inventory information, and fragility formulations that are methodologically consistent with prior Istanbul applications.

Second, the analytical emphasis shifts from estimating absolute loss quantities to identifying statistically coherent neighborhood scale risk profiles. The objective is not to generate new deterministic damage scenarios, but to structure existing loss outputs into empirically validated typologies that are interpretable and operationally meaningful.

Methodologically, the contribution lies in the structured integration of model comparison, multi criteria selection procedures, and formal stability assessment within the context of an official urban loss database. While the clustering algorithms themselves are well established, their systematic application to neighborhood level loss indicators, combined with explicit evaluation of partition robustness, extends prior Istanbul studies. Earlier scenario-based assessments did not quantify the reproducibility of spatial loss groupings through resampling based stability metrics or consensus analysis. By incorporating these procedures, the present study demonstrates that the distinction between High Impact and Low Impact neighborhood profiles reflects a statistically coherent and reproducible structure rather than an artifact of arbitrary classification choices.

5.2. Neighborhood scale, within-district heterogeneity, and aggregation

https://doi.org/10.48088/ejg.r.avc.17.1.017.034

District level maps often provide a simplified representation of spatial risk, yet such aggregation can obscure substantial heterogeneity within administrative boundaries. The findings of this study support this concern. Neighborhoods classified as High Impact and Low Impact frequently coexist within the same district, especially in larger districts characterized by mixed land use patterns and diverse building stocks. This internal variability indicates that district level averages may conceal meaningful contrasts at finer spatial resolution.

District summaries, such as the proportion of High Impact neighborhoods within each district, can still serve a communicative purpose. They offer a broad overview and may facilitate dialogue at administrative levels where district units are commonly used. However, these summaries do not replace neighborhood level classification. The analytical procedure and clustering were conducted exclusively at the neighborhood scale, and interpretation of risk differentiation remains anchored at that level.

Aggregation to the district scale is therefore treated as a descriptive extension rather than as the primary unit of analysis. By explicitly distinguishing between the scale of clustering and the scale of optional reporting, the study addresses concerns related to ecological fallacy and scale mismatch. The results demonstrate that meaningful risk differentiation emerges at the neighborhood level and that this differentiation may be diluted if interpreted solely through district averages.

5.3. Links to geological conditions and building-stock characteristics

The clustering procedure relies on outcome indicators, namely expected structural damage and human losses, rather than on explicit geological or structural input variables. Nevertheless, the spatial configuration of the resulting profiles shows a clear and interpretable correspondence with established seismic risk determinants.

High Impact neighborhoods are predominantly concentrated along the Sea of Marmara coastal corridor. These areas are widely characterized by soft alluvial deposits and artificial fill zones, where basin effects and site amplification mechanisms are known to increase ground motion intensity. In addition, many neighborhoods in this belt contain relatively older building stock constructed before the implementation and enforcement of more recent seismic design regulations.

In contrast, Low Impact neighborhoods are more common in northern districts associated with comparatively favorable site conditions and newer development patterns. Buildings in these areas are more likely to have been designed under updated seismic codes. Lower development density and differing land use configurations may also contribute to the reduced expected impacts observed in these neighborhoods.

The distinction between High Impact and Low Impact profiles therefore cannot be reduced to a simple relationship between building counts and risk magnitude. Instead, the classification reflects a compounded outcome that integrates hazard intensity, exposure, and structural vulnerability as embedded in the underlying scenario framework. The loss estimation model already accounts for geological conditions through ground motion modeling and amplification effects, and for building characteristics through typology specific fragility formulations. The clustering analysis reorganizes these combined influences into coherent and reproducible spatial groups.

Future research may further clarify these linkages by directly overlaying cluster classifications with geological units, soil classes, and building age distributions, thereby enabling a more explicit examination of the structural drivers underlying the observed profiles.

5.4. Implications for urban planning and emergency management

The binary classification of neighborhoods into High Impact and Low Impact groups has several practical implications for urban planning and disaster management.

First, the High Impact cluster provides a clear basis for prioritizing structural risk reduction efforts. Neighborhoods in this group may be considered primary candidates for detailed field surveys, structural screening programs, retrofitting initiatives, and where relevant, renewal interventions. The identified medoid neighborhoods can serve as pilot locations for testing intervention strategies and refining technical and organizational procedures before broader implementation across the cluster.

Second, emergency preparedness strategies may benefit from incorporating the spatial concentration of High Impact neighborhoods. The pre-positioning of shelters, temporary medical facilities, search and rescue teams, and logistical assets in proximity to these areas can contribute to shorter response times and improved allocation efficiency during

a major event. Resource allocation can thus be aligned with expected operational demand derived from scenario-based impact estimates.

Third, risk communication and community preparedness initiatives can be differentiated according to cluster membership. High Impact neighborhoods may require more intensive outreach and awareness programs, while Low Impact areas can focus on maintaining existing safety standards and preventing risk accumulation through ongoing development processes.

Fourth, the cluster classification can be integrated with additional planning layers. Joint evaluation with socio economic vulnerability indicators, infrastructure criticality assessments, and transportation accessibility metrics would enable a more comprehensive resilience-oriented planning framework.

For High Impact neighborhoods in particular, mitigation policies may emphasize structural upgrading of older building stock and careful management of development intensity in areas characterized by soft soil conditions. In contrast, Low Impact neighborhoods, especially in northern districts, may represent relatively suitable zones for logistical coordination and temporary shelter planning, provided that future development remains consistent with seismic safety principles.

Although the distinction between High Impact and Low Impact profiles offers a simplified structure for communication with non-technical stakeholders, it is derived from a systematic statistical synthesis of scenario-based impact indicators. The typology therefore balances interpretability with methodological rigor.

5.5. Limitations and future research

Several limitations should be considered when interpreting the findings of this study. First, the analysis is based on a single deterministic Mw 7.5 earthquake scenario. Alternative rupture geometries, magnitude levels, or assumptions regarding the time of occurrence may produce different distributions of damage and casualties. Extending the framework to incorporate multiple rupture scenarios and probabilistic hazard representations would allow evaluation of the robustness of the identified cluster structure under varying seismic conditions.

Second, the clustering procedure relies exclusively on structural damage and direct human impact indicators. Broader dimensions of risk and resilience, such as socio-economic vulnerability, functional disruption, infrastructure interdependencies, and post event recovery capacity, are not explicitly included. Integrating such variables would enable a more comprehensive assessment of urban resilience and may reveal additional layers of spatial differentiation (e.g., Adu-Gyamfi & Shaw, 2021; Ghaffarian et al., 2025; Kalaycıoğlu et al., 2023).

Third, the selection of a two-cluster configuration reflects a deliberate balance among interpretability, internal validity, and stability. More detailed partitions could potentially capture additional variation within the dataset. However, given the current indicators and sample structure, solutions with higher k values exhibit reduced stability and less coherent separation. Future studies that incorporate enriched indicator sets or expanded temporal and spatial data may revisit the determination of the optimal number of clusters.

Despite these constraints, the proposed framework offers a transparent and reproducible approach to neighborhood scale seismic risk profiling. By combining internal validation, stability assessment, and interpretable cluster representation, the study establishes a methodological baseline that can be extended and refined in subsequent research.

6. Conclusions

This study develops a data driven classification of earthquake impact profiles for the 959 neighborhoods of Istanbul under the official Mw 7.5 nighttime scenario. Through systematic preprocessing, principal component-based dimensionality reduction, comparative evaluation of alternative clustering algorithms, and formal stability assessment, the analysis identifies two statistically coherent and operationally meaningful profiles.

The first profile corresponds to neighborhoods with systematically higher expected building damage and human losses. These High Impact areas are concentrated primarily along the Sea of Marmara coastal corridor and within older and denser urban zones. The second profile consists of neighborhoods with comparatively lower expected impacts, more prevalent in northern districts and in areas characterized by newer development patterns. Bootstrap results, with a mean Adjusted Rand Index of 0.976, indicate a high level of reproducibility for the two-cluster configuration. The spatial coherence of the resulting profiles further supports the interpretation that the classification reflects a structured feature of the scenario dataset rather than instability arising from sampling or initialization effects.

https://doi.org/10.48088/ejg.r.avc.17.1.017.034

An additional contribution lies in the use of medoid neighborhoods as concrete representatives of each profile. Because cluster centers correspond to actual neighborhoods, the High Impact and Low Impact groups are linked to identifiable reference cases. In this study, Fatih Nişanca and Çekmeköy Sultançiftliği serve as interpretable prototypes. These neighborhoods provide tangible starting points for the design and testing of mitigation and preparedness measures that can subsequently be extended to other areas with similar impact characteristics.

Overall, the findings illustrate how unsupervised learning methods, when embedded within a transparent validation framework and applied to up-to-date scenario-based loss data, can support neighborhood scale earthquake risk management. By combining statistical rigor with practical interpretability, the proposed typology complements existing district level assessments and contributes to more targeted and evidence-based planning strategies in Istanbul.

Funding: This research received no external funding.

Conflicts of Interest: The authors declare no conflict of interest.

Acknowledgments: The authors are grateful to the anonymous reviewers for their constructive feedback, which helped strengthen the clarity and rigor of this study.

Data Availability Statement: The data used in this study are derived from the official outputs of the Istanbul Province Possible Earthquake Loss Estimates Update Project conducted by the Istanbul Metropolitan Municipality and Kandilli Observatory and Earthquake Research Institute, initiated in 2019 and disseminated between 2019 and 2023. The relevant datasets are publicly available through the Deprem Zemin project web pages and the asso-ciated district level loss estimate booklets published by the Istanbul Metropolitan Municipality (Istanbul Metropolitan Municipality, n.d.-a, n.d.-b).

Appendix

Table A1. Nonparametric significance test and effect size for differences between clusters

Indicator	p-value (Mann–Whitney U tests)	Cliff's δ
Bina_1	$< 10^{-6}$	0.8086
Bina_2	$< 10^{-6}$	0.8589
Bina_3	$< 10^{-6}$	0.8884
Bina_4	$< 10^{-6}$	0.9100
HumanImpact_1	$< 10^{-6}$	0.9797
HumanImpact_2	$< 10^{-6}$	0.9893
HumanImpact_3	$< 10^{-6}$	0.9810
HumanImpact_4	$< 10^{-6}$	0.9891

References

Adu-Gyamfi, B., & Shaw, R. (2021). Utilizing population distribution patterns for disaster vulnerability assessment: Case of foreign residents in the Tokyo Metropolitan Area of Japan. *International Journal of Environmental Research and Public Health, 18*(8), Article 4061. https://doi.org/10.3390/ijerph18084061

Ansal, A., Akinci, A., Cultrera, G., Erdik, M., Pessina, V., Tönük, G., & Ameri, G. (2009). Loss estimation in Istanbul based on deterministic earthquake scenarios of the Marmara Sea region (Turkey). *Soil Dynamics and Earthquake Engineering, 29*(4), 699–709. https://doi.org/10.1016/j.soildyn.2008.07.006

Caliński, T., & Harabasz, J. (1974). A dendrite method for cluster analysis. *Communications in Statistics—Theory and Methods, 3*(1), 1–27. https://doi.org/10.1080/03610927408827101

Campello, R. J. G. B., Moulavi, D., Zimek, A., & Sander, J. (2015). Hierarchical density estimates for data clustering, visualization, and outlier detection. *ACM Transactions on Knowledge Discovery from Data,* 10(1), Article 5, 1–51. https://doi.org/10.1145/2733381

Davies, D. L., & Bouldin, D. W. (1979). A cluster separation measure. *IEEE Transactions on Pattern Analysis and Machine Intelligence, 1*(2), 224–227. https://doi.org/10.1109/TPAMI.1979.4766909

Erdik, M., Aydinoglu, N., Fahjan, Y., Sesetyan, K., Demircioglu, M., Siyahi, B., Durukal, E., Ozbey, C., Biro, Y., Akman, H., & Yuzugullu, O. (2003). Earthquake risk assessment for Istanbul metropolitan area. *Earthquake Engineering and Engineering Vibration, 2*(1), 1–23. https://doi.org/10.1007/BF02857534

Erdik, M., Hancılar, U., & Tüzün, C. (2010). ELER software—A new tool for urban earthquake loss assessment. *Natural Hazards and Earth System Sciences, 10(*12), 2677–2696. https://doi.org/10.5194/nhess-10-2677-2010

Ersoz, T., & Bayrak, G. (2023). Investigation of possible earthquake risk in districts of istanbul using the Fine-Kinney method. Uluslararası Sürdürülebilir Mühendislik ve Teknoloji Dergisi, 7(2), 139-151. https://izlik.org/JA67AP77YG

Fraley, C., & Raftery, A. E. (2002). Model-Based Clustering, Discriminant Analysis, and Density Estimation. *Journal of the American Statistical Association,* 97(458), 611–631. https://doi.org/10.1198/016214502760047131

Ghaffarian, S., Shafapourtehrany, M., Lagap, U. (2025). Earthquake-based multi-hazard resilience assessment: a case study of Istanbul, Turkey (neighborhood level). *npj Nat. Hazard,* 2, 15. https://doi.org/10.1038/s44304-025-00065-8

Gürfidan, S., & Yalçınkaya, A. (2024). Scenario-based estimation of earthquake fatalities for Istanbul using machine learning. *Karaelmas Fen ve Mühendislik Dergisi, 14*(1), 23–33. https://doi.org/10.7212/karaelmasfen.1494349

Hubert, L., & Arabie, P. (1985). Comparing partitions. *Journal of Classification, 2*, 193–218. https://doi.org/10.1007/BF01908075

Istanbul Metropolitan Municipality. (n.d.-a). Istanbul Province Possible Earthquake Loss Estimates Update Project (2019). *Deprem Zemin*. https://depremzemin.ibb.istanbul/en/istanbul-province-possible-earthquake-loss-estimates-update-project

Istanbul Metropolitan Municipality. (n.d.-b). Possible Earthquake Loss Estimates District Booklets. *Deprem Zemin*. https://depremzemin.ibb.istanbul/en/possible-earthquake-loss-estimates-district-booklets

Jain, A. K. (2010). Data clustering: 50 years beyond k-means. *Pattern Recognition Letters, 31*(8), 651–666. https://doi.org/10.1016/j.patrec.2009.09.011

Jena, R. K., Pradhan, B., Beydoun, G., Alamri, A. M., & Sofyan, H. (2020). Earthquake hazard and risk assessment using machine learning approaches at Palu, Indonesia. *Science of the Total Environment, 749*, Article 141582. https://doi.org/10.1016/j.scitotenv.2020.141582

Jolliffe, I. T. (2002). *Principal component analysis (2nd ed.).* Springer.

Kalaycıoğlu, E., Tanganelli, M., Viti, S., & Martinelli, E. (2023). Social vulnerability and urban resilience assessment for Istanbul: A neighborhood-scale approach. *Natural Hazards and Earth System Sciences, 23*(7), 2563–2583. https://doi.org/10.5194/nhess-23-2563-2023

Kalaycıoğlu, O., Akhanlı, S. E., Menteşe, E. Y., Kalaycıoğlu, M., & Kalaycıoğlu, S. (2023). Using machine learning algorithms to identify predictors of social vulnerability in the event of a hazard: Istanbul case study. *Natural Hazards and Earth System Sciences, 23*(6), 2133–2156. https://doi.org/10.5194/nhess-23-2133-2023

Kalkan, E., Gülkan, P., Yılmaz, N., & Çelebi, M. (2009). Reassessment of probabilistic seismic hazard in the Marmara Region. *Bulletin of the Seismological Society of America, 99*(4), 2127–2146. https://doi.org/10.1785/0120080285

Kaufman, L., & Rousseeuw, P. J. (1990). Finding groups in data: An introduction to cluster analysis. *Wiley*.

Li, Y., Zhai, G., Huang, Q., Liu, Y., & Chen, J. (2016). Measuring county resilience after the 2008 Wenchuan earthquake. *International Journal of Disaster Risk Science, 7*(4), 393–412. https://doi.org/10.1007/s13753-016-0109-2

MacQueen, J. (1967). Some methods for classification and analysis of multivariate observations. In *Proceedings of the Fifth Berkeley Symposium on Mathematical Statistics and Probability* (Vol. 1, pp. 281–297). University of California Press. http://projecteuclid.org/euclid.bsmsp/1200512992

Monti, S., Tamayo, P., Mesirov, J., & Golub, T. (2003). Consensus clustering: A resampling-based method for class discovery and visualization of gene expression microarray data. *Machine Learning, 52, 91*–118. https://doi.org/10.1023/A:1023949509487

Ng, A. Y., Jordan, M. I., & Weiss, Y. (2002). On spectral clustering: Analysis and an algorithm. *Advances in Neural Information Processing Systems,* 14, 849-856.

Rousseeuw, P. J. (1987). Silhouettes: A graphical aid to the interpretation and validation of cluster analysis. *Journal of Computational and Applied Mathematics, 20, 53–65.* https://doi.org/10.1016/0377-0427(87)90125-7

Olivares-Palomares, Á. B., Aguirre, J., & Ramírez-Guzmán, L. (2025). Southern Mexico City shear-wave velocity estimation using ambient seismic noise. *Seismological Research Letters*. https://doi.org/10.1785/0220240488

Tibshirani, R., Walther, G., & Hastie, T. (2001). Estimating the number of clusters in a dataset via the gap statistic. *Journal of the Royal Statistical Society: Series B (Statistical Methodology), 63(2)*, 411–423. https://doi.org/10.1111/1467-9868.00293

Xu, R., & Wunsch, D. I. (2005). Survey of clustering algorithms. *IEEE Transactions on Neural Networks, 16*(3), 645–678. https://doi.org/10.1109/TNN.2005.845141

Von Luxburg, U. (2010). Clustering stability: An overview. *Foundations and Trends in Machine Learning*, 2(3), 235–274. https://doi.org/10.1561/2200000018

Yeo, I.-K., & Johnson, R. A. (2000). A new family of power transformations to improve normality or symmetry. *Biometrika*, 87(4), 954–959. https://doi.org/10.1093/biomet/87.4.954

European Journal of Geography